Exploring Photophysical Properties and Sensitivity to Dioxygen in Anisolyl-Picolinate Antenna Conjugated to Azamacrocycles

Lucile Bridou,[a] Loëza Collobert,[b] Kyangwi P. Malikidogo,[c] Salauat R. Kiraev,[a] Maher Hojorat,[a] Nadège Hamon,[b] Anh Thy Bui,[d] François Riobé,[e] Akos Banyasz,[a] Maryline Beyler,[b] Raphaël Tripier,[b,*] Olivier Sénèque,[c,*] Olivier Maury[a,*]

[a] Dr. L. Bridou, Dr. M. Hojorat, Dr. S.R. Kiraev, Dr. A. Banyasz, Dr O. Maury
CNRS, ENS de Lyon, LCH UMR 5182, 69342 Lyon cedex 07, France

[b] L. Collobert, Dr. M. Beyler, Prof. R. Tripier
Univ Brest, UMR CNRS 6521 CEMCA, F-29200 Brest, France.

[c] Dr. K. P. Malikidogo, Dr. O. Sénèque
Univ. Grenoble Alpes, CNRS, CEA, IRIG, LCBM (UMR 5249), F-38000 Grenoble, France

[d] Dr. A.T. Bui
Univ. Bordeaux, CNRS, Bordeaux INP, ISM, UMR 5255, F-33400 Talence, France

[e] Dr. F. Riobé
Univ. Bordeaux, CNRS, Bordeaux INP, ICMCB UMR 5026, F-33600 Pessac, France

TOC abstract

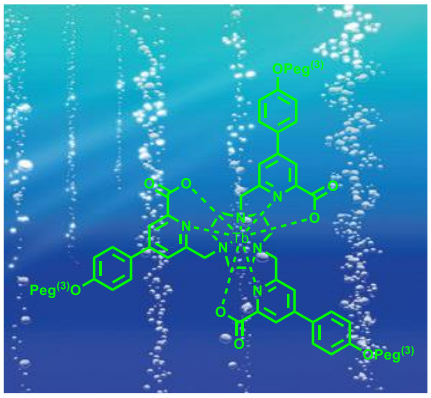

Abstract

An anisolyl-picolinate antenna grafted onto different macrocyclic ligands such as tacn, pyclen or cyclen renders the resulting terbium (III) complexes highly sensitive towards oxygen in aqueous solutions, enabling the design of ratiometric or lifetime-based molecular sensors. The underlying sensitization mechanism was investigated on analogous Gd(III) complexes and the oxygen sensitivity was studied using transient absorption spectroscopy. The antenna-based triplet lifetime increased up to 900-fold upon degassing, underscoring the role of the ligand excited states in designing highly sensitive oxygen probes.

Introduction

The detection and control of dioxygen concentration are crucial in various fields, including industrial chemistry, agri-food, environmental sciences, and clinical analysis.[1-3] As an example, molecular oxygen plays a key role in biological processes, making its detection important to understand physiological and pathological phenomena. Among all existing techniques (the Winkler, amperometric and pressure-based methods), optical methods offer a non-invasive and precise alternative for dioxygen detection, with advantages such as rapid response, high sensitivity, and ease of miniaturization, leading to an increased interest in the design of optical dioxygen molecular sensors.[4]

Since the seminal discovery of Kautsky and Hirsch in 1931,[5] it is well established that emission and, more particularly, phosphorescence emission of chromophores decreases in the presence of dioxygen. This reversible photophysical process involves a collisional deactivation of the chromophore triplet excited state by dioxygen in its fundamental triplet state ($^3\Sigma$).[6] This process may lead to the formation of singlet oxygen ($^1\Delta$), which is detectable through its characteristic luminescence emission or by using a scavenger. The high cytotoxicity of these species is instrumental in the development of photodynamic therapy (PDT) applications.[7, 8] In addition, the decrease of luminescence intensity and lifetime provides measurable parameters for dioxygen detection. Consequently, the (I_0/I) and (τ_0/τ) ratios, where I_0 and I (respectively, τ_0 and τ) are the luminescence intensities (respectively, lifetimes) in the absence and in the presence of O_2, can conveniently provide an evaluation of molecular probe sensitivity.

Cross-solvent comparisons can be conducted using the Stern-Volmer equation (1), which relates the luminescence intensity and lifetime to the dioxygen concentration: [4]

$$(1)\quad \frac{I_0}{I} = \frac{\tau_0}{\tau} = 1 + K_{SV}[O_2]$$

The Stern-Volmer constant K_{SV} reveals the efficiency of luminescence quenching, or the accessibility of the fluorophores to the quencher. Phosphorescence-based sensors often exhibit very high K_{SV} values, and consequently dioxygen-sensitive probes based on polycyclic aromatic hydrocarbons (pyrene, anthracene, perylene etc...), quinone or erythrosine are frequently described in the literature.[4] Increasing the lifetime of the probe to favor collisional quenching by dioxygen in the excited state appears to be a straightforward strategy to improve the sensitivity. This has led to the development of transition metal-based molecular probes, among which ruthenium(II) polypyridine and platinum or palladium(II) metalloporphyrins are known to present the highest K_{SV} values (up to 10000 M^{-1}). These structures are now ubiquitous in the design of dioxygen sensors or molecular photosensitizers for PDT applications.[9]

This decade, lanthanide complexes have made a significant breakthrough in this field driven by the efforts of several groups such as those led by Parker, Faulkner, Wang, Wong, De Bettencourt-Dias, Kitagawa and Hasegawa and our consortium, and they were recently reviewed in the scope of oxygen sensitivity and PDT.[10, 11] On the one hand, Gd(III) complexes, known to promote the formation ligand-centered triplet exited state by heavy atom effect, act as straightforward sensitizer for the generation of singlet oxygen with promising applications in PDT, [12-18] as well as for the design of theranostic magnetic resonance imaging (MRI) and PDT probes. [19-21] On the other hand, emissive lanthanide ions (mainly Tb(III) and to a lesser extent Dy(III), Eu(III)

and Yb(III)), have been used for the design of dioxygen-sensitive luminescent sensors.[10] In this case, the emission quenching mechanism is slightly more complicated than in organic or transition metal complexes: the sensitization of lanthanide luminescence is generally achieved via an antenna effect from the organic ligand triplet state.[22] This intramolecular photophysical process is typically much faster than the intermolecular dioxygen collisional quenching process. However, in some particular cases, where the energy gap between the lanthanide accepting level and the triplet excited state is smaller than 2000 cm^{-1}, a thermally-activated back energy transfer (BET) is possible, resulting in a long-lived excited state equilibrium. This situation enables triplet state quenching by dioxygen that translates into a decrease in the luminescence intensity or lifetime of the lanthanide center.[23-28] Therefore, by fine-tuning the ligand triplet energy level, it is possible to devise lanthanide-based dioxygen sensors. As an example, Nakai et al. reported very sensitive Tb(III) complexes featuring aryloxy antennas **$[TbL_0]^-$** (figure 1) with exceptional *apparent* K_{sv} constants up to 17000 M^{-1} (Figure 1).[29-31] In the particular case of lanthanide luminescent oxygen sensors, the K_{sv} constant is considered as *apparent* due to the luminescent state being localized on the lanthanide ion, while the excited state involved in quenching by oxygen is the antenna ligand triplet. The application of the Stern-Volmer formalism to these systems requires the assumption that the sensitization and backward energy transfer pathways are much faster than oxygen quenching processes.[32]

During the course of our quest for the new π-conjugated chromophores sensitizing lanthanide emission, we reported the design of tacn-based Tb(III) complexes featuring two different anisolyl-picolinate antennas: unsubstituted **$[TbL_1]$**[33] and with a methyl group at the *ortho*-position **$[TbL_{1Me}]$**[34] (Figure 1). The effect of this small substituent on the photophysical properties was drastic, considering **$[TbL_{1Me}]$** exhibited a very high quantum yield (Φ = 0.75 in H_2O), while **$[TbL_1]$** showed rather modest luminescence properties (Φ = 0.30 in H_2O). To rationalize this difference, the luminescence of **$[TbL_1]$** was initially proposed to be dependent on the viscosity of the surrounding medium.[33] However, Parker and coworkers demonstrated that this interpretation was incorrect and **$[TbL_1]$** was in fact very sensitive to dioxygen.[35, 36] In this article, we thoroughly explore the photophysical properties of the anisolyl-picolinate antenna linked to tacn (1,4,7-triazacyclononane), as well as pyclen (3,6,9,15-tetraazabicyclo[9.3.1]pentadeca-1(15),11,13-triene) and cyclen (1,4,7,10-tetraazacyclododecane)-based macrocycles (Figure 1). All Tb(III) complexes appeared to be highly sensitive to dioxygen, while Eu(III) complexes were not. This behavior was utilized in the conception of a ratiometric system for dioxygen sensing. In addition, the photophysical sensitization mechanism was investigated by means of transient absorption spectroscopy using the related gadolinium complexes, confirming the exceptional sensitivity of the ligand-centered triplet state to dioxygen.

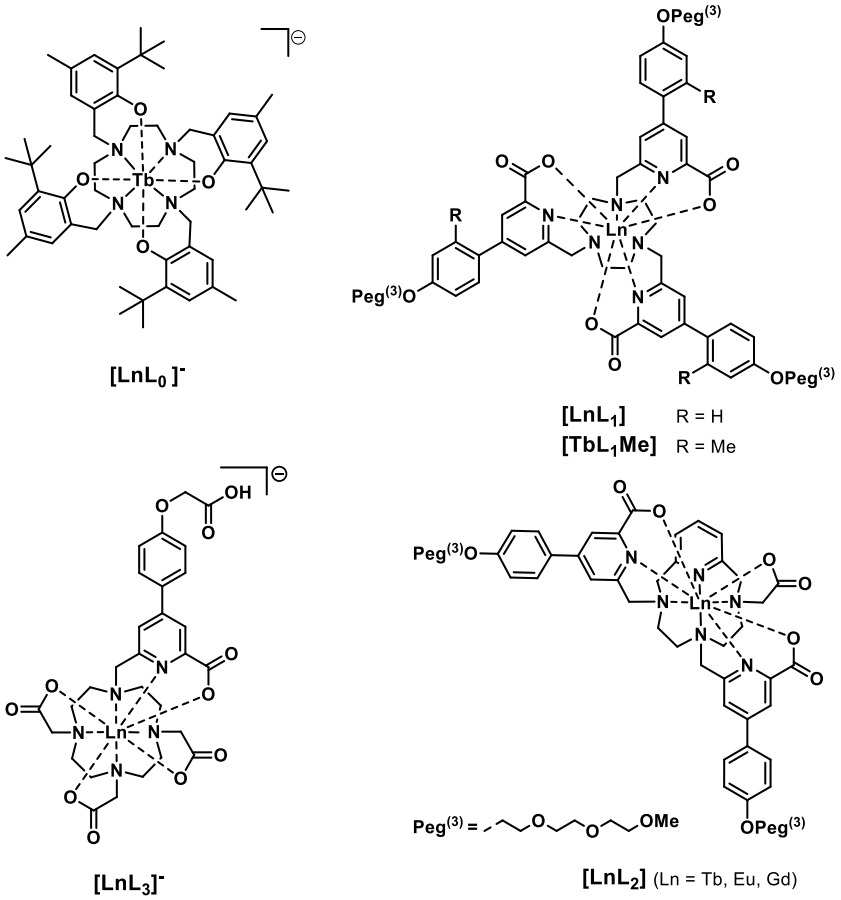

Figure 1. Structures of O_2-sensitive Tb(III) complexes.

RESULTS AND DISCUSSION

Synthesis. The mesylated anisolyl-picolinate antenna (**1**), the corresponding tacn-based methyl ester protected ligand $\mathbf{L_1}$, and the [Ln$\mathbf{L_1}$] complexes (Ln = Eu, Gd and Tb) were synthesized as previously described by some of us.[33] The antenna **1** was also introduced on a pyclen scaffold (Scheme 1). Pyclen mono-acetate protected in its methyl ester form (**2**) was prepared using a *N*-regioselective functionalization strategy already reported in the literature. [37, 38] Pyclen derivative **2** underwent a nucleophilic substitution reaction with antenna **1** (2 equiv.) in the presence of potassium carbonate in acetonitrile to give pro-ligand $\mathbf{L_2}$' with 76% yield. The methyl ester function of $\mathbf{L_2}$' was subjected to basic hydrolysis (KOH, 1M). The resulting ligand $\mathbf{L_2}$ was directly reacted with 1.2 equivalents of $LnCl_3.6H_2O$ (Ln = Gd, Tb) at pH ~ 6. After removal of the inorganic salts in methanol, the **[Ln$\mathbf{L_2}$]** complexes were isolated in near-quantitative yields (Scheme 1).

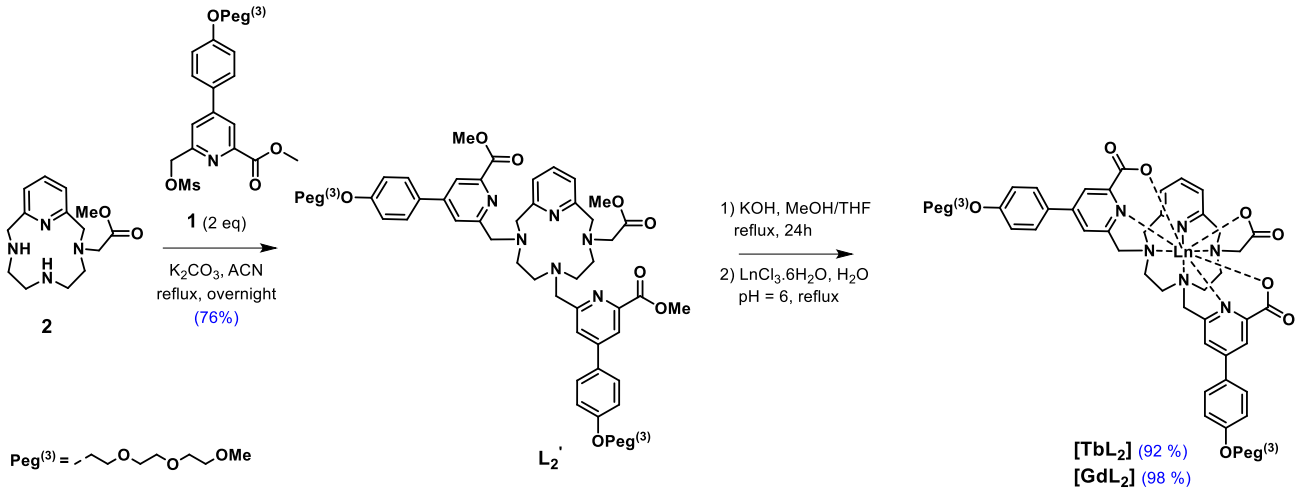

Scheme 1. Synthetic pathway for **[LnL$_2$]** complexes.

In the case of the cyclen macrocycle, a more divergent synthetic strategy was employed using the iodinated precursor **3** (Scheme 2).[39] A Suzuki-Miyaura cross-coupling between **3** and **4**, followed by basic hydrolysis of the methyl and acidolysis of the *tert*-butyl esters afforded ligand **L$_3$** after HPLC purification in an excellent 80% yield. Metalation using $LnCl_3$ (Ln = Eu, Gd, Tb) was performed in water at pH 6. The compounds were characterized by NMR and/or HR/MS and the purity of the Ln(III) complexes was assessed by analytical HPLC. All synthetic procedures and characterizations are detailed in the Supporting Information (Scheme S1-2).

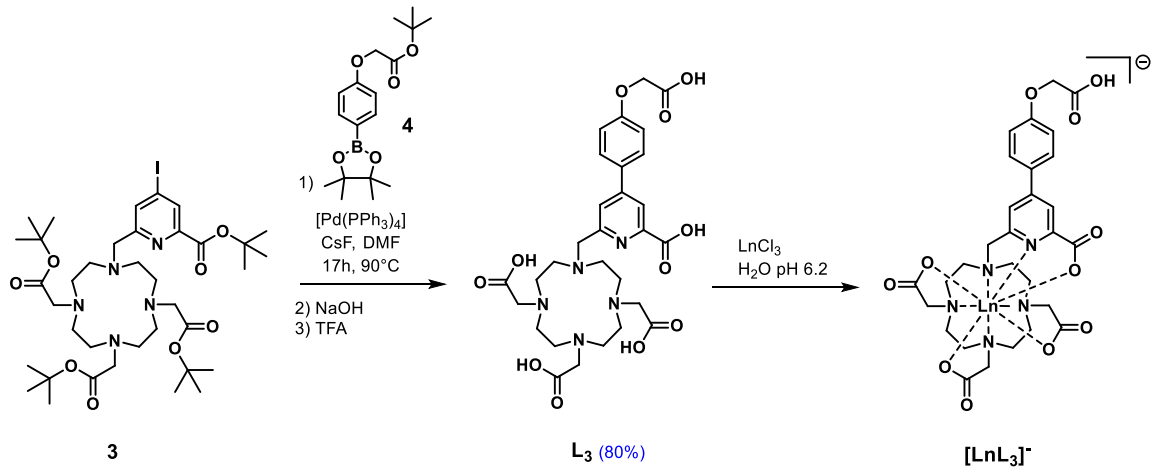

Scheme 1. Synthetic pathway for **[LnL$_3$]$^-$** complexes.

Photophysical properties. The photophysical properties of the different complexes were measured in diluted aqueous media (water or PBS buffer). All complexes exhibited a broad absorption band centered at 304-308 nm with a cut-off wavelength at 360 nm assigned to an Intra-Ligand Charge Transfer (ILCT) transition from the anisole donor moiety to the central pyridine moiety (Table 1). The absorption spectra were very similar for all types of macrocycles, the molar extinction coefficient increasing with the number of antennas per Ln(III) complex. Emission properties were studied either in air-equilibrated or in degassed media. The degassing process was rigorously carried out using a freeze-pump-thaw technique for three cycles and the final solution was then stored under argon in a custom cuvette equipped with a J. Young valve (see SI for details). Upon

excitation in the ILCT bands, characteristic Tb(III) emission profiles attributed to the $^5D_4 \rightarrow {}^7F_J$ (J =6-0) transitions were observed for the three **[TbL$_i$]** (i = 1-3) complexes (Figure 2). The emission profiles were very similar for the three complexes since the luminescence of Tb(III) is little affected by coordination geometry. Quantum yields and lifetimes have been measured for the whole series and are reported in Table 1. All Tb(III) complexes were sufficiently emissive with quantum yields varying between 28 and 40%. Upon degassing, the luminescence intensity increased strongly and the final quantum yield more than doubled (in the 68-76% range). Luminescence lifetimes mirrored the behavior observed in light emission intensity. As an example, the lifetime value of **[TbL$_1$]** featuring three antennas increased from 0.45 under air to 1.28 ms after degassing, while the quantum yield increased from 30 to 75%. As all parameters (concentration, solvent, and temperature) were kept constant between the two measurements, this result indicates that the presence of air, and in particular dioxygen, is responsible for the main non-radiative deactivation process. In order to compare the relative sensitivity of the different macrocycles, we calculated the ratios τ^0/τ and Φ^0/Φ of the values measured in degassed and air-equilibrated media (Table 1). As expected, for a given complex, both ratios are identical within the experimental error. **[TbL$_1$]** and **[TbL$_3$]$^-$** clearly exhibit comparable sensitivity to dioxygen, significantly higher than that of the pyclen-based **[TbL$_2$]**, and the relative sensitivities determined in luminescence lifetimes are slightly higher than using quantum yields.

The photophysical properties of analogous **[EuL$_1$]** and **[EuL$_3$]$^-$** were also determined (Figure 3). Unsurprisingly, the Eu(III) complexes were more sensitive to the local symmetry, resulting in very different emission spectral profiles.[40] However, in both cases, the luminescence quantum yields and lifetimes were identical in degassed and air-equilibrated media, indicating that no dioxygen quenching process is at play.

Table 1. Photophysical properties of **[TbL$_1$]**, **[TbL$_2$]**, **[TbL$_3$]$^-$**, **[EuL$_1$]** in water and **[EuL$_3$]$^-$** in PBS. The 0 superscript denotes degassed solutions.

Complex	λ_{max}^{abs} (nm)	ε_{max} ($M^{-1}.cm^{-1}$)	τ (ms)	τ^0 (ms)	Φ[a]	Φ^0 [b]	τ^0/τ	Φ^0/Φ
[TbL$_1$]	308	47 000	0.45	1.28	0.30	0.75	2.8	2.5
[TbL$_2$]	304	43 000	0.71	1.41	0.40	0.76	2.0	1.9
[TbL$_3$]$^-$	307	20 000	0.88	2.29	0.28	0.68	2.6	2.4
[EuL$_1$]	308	50 000	0.83	0.85	0.25	0.26	1.0	1.0
[EuL$_3$]$^-$	307	20 000	1.11	1.11	0.14	0.14	1.0	1.0

[a] Determined by relative method using quinine bisulfate in 1 N H_2SO_4 as reference.

[b] Determined by a single measurement, using the quantum yield value obtained for the same compound in aerated solvent as reference.

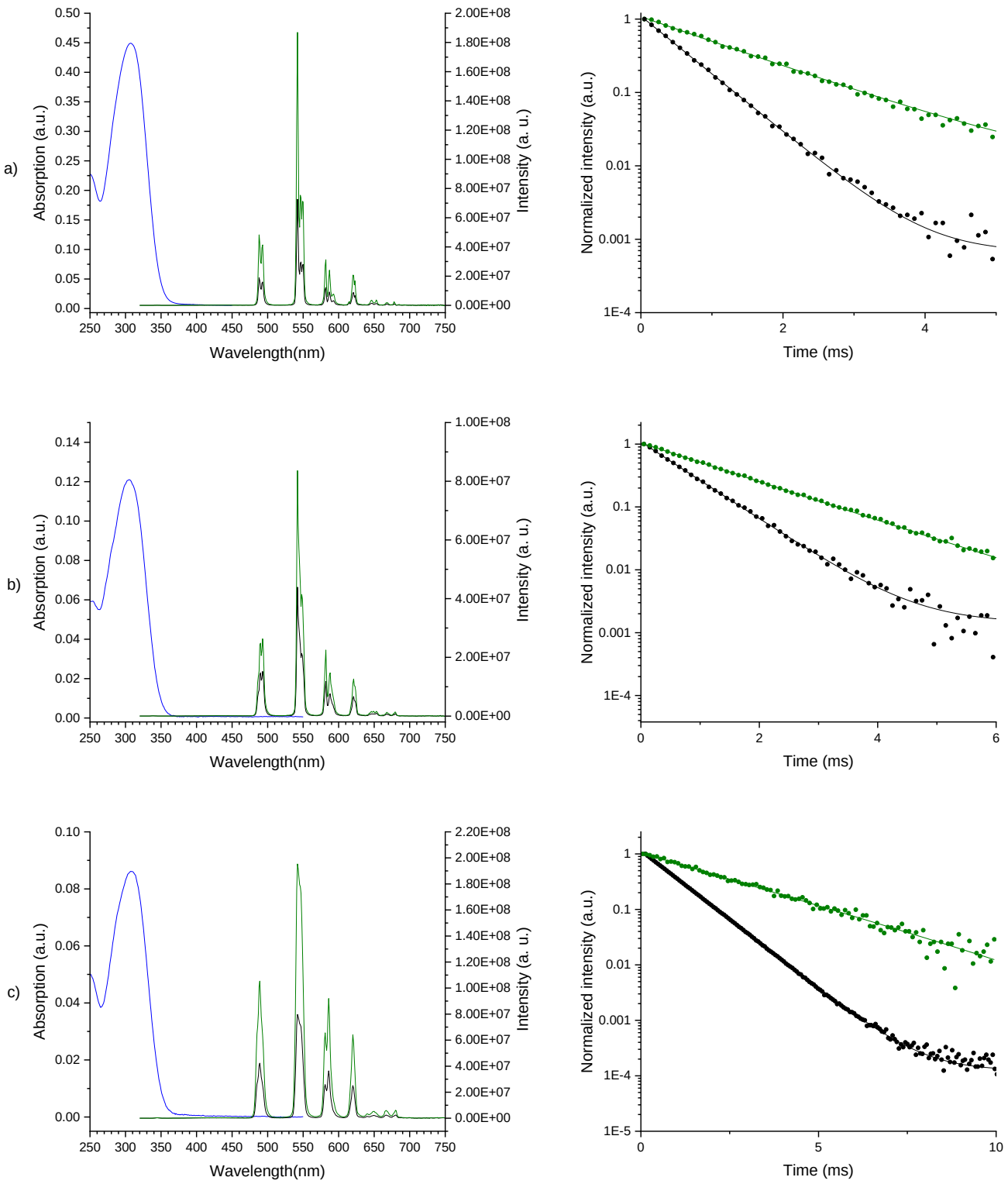

Figure 2. Left: Absorption (blue) and emission spectra (λ_{ex} = 307 nm) measured in aerated (black) and degassed (green) H_2O. Right: lifetime measurement (λ_{ex} = 307 nm, λ_{em} = 541 nm) in aerated (black) and deoxygenated water (green). Spots: experimental data, line: exponential fit. a**) [TbL$_1$]**, b) **[TbL$_2$]** and, c) **[TbL$_3$]**$^-$

.

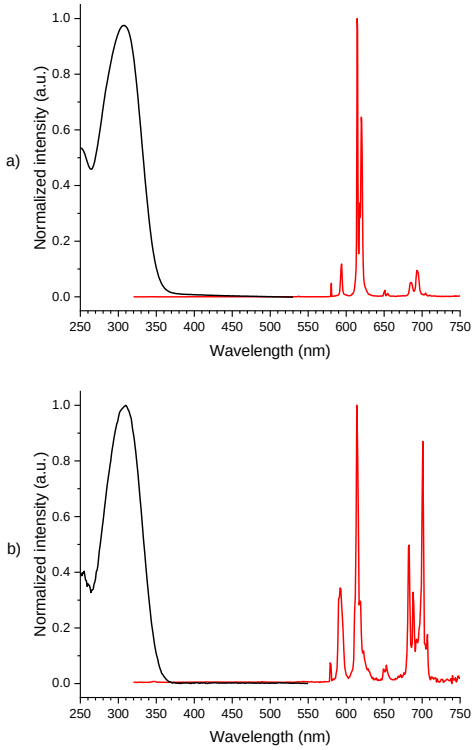

Figure 3. Absorption (black) and emission spectra (red, λ_{ex} = 307 nm) measured in H_2O for a) [Eu**L$_1$**], and b) [Eu**L$_3$**]$^-$.

These results indicated that for a given ILCT antenna, the spectroscopic behavior of the Tb(III) or Eu(III) complexes are identical regardless of the macrocycle nature. With the present anisolyl-picolinate antenna, the terbium complexes exhibited a strong sensitivity towards dioxygen, while the luminescence of europium complexes were independent of the dioxygen concentration. This condition is the perfect requirement for the design of ratiometric probes for the detection of dioxygen and the quantification of its concentration in solution. Therefore, we measured the luminescence variations of an aqueous solution of **[TbL$_1$]** and **[EuL$_1$]** (2:1 mixture) as a function of dissolved dioxygen concentration, which was independently determined by a specific oxygen electrode (see SI for details). As illustrated in Figure 4, the Tb(III) signal decreases as the dioxygen concentration increases, while the Eu(III) signal remained constant and could be used as an internal standard. The ratio between the emission intensities of Tb(III) and Eu(III) ($\Delta = I_{542}/I_{614}$), measured at 542 nm and 614 nm, respectively, varies linearly with the dioxygen concentration in solution (Figure 4b). This calibration plot allows the determination of dioxygen concentration in a solution with an unknown amount of dissolved O_2. Likewise, the Tb(III) luminescence lifetime also varied linearly with oxygen concentration in water (in the studied range), in the case of **[TbL$_1$]** (Figure S2). The Stern-Volmer equation (1) could be applied to determine the sensitivity of the probe. In the present case, τ_0 was previously determined to be 1.28 ms using freeze-pump-thaw technique and using Figure 5, we estimated the *apparent* Stern-Volmer constant K_{SV} = 4700 M^{-1}. This sensitivity was of the same order of magnitude as that of classical tris-bipyridyl ruthenium(II) or porphyrine-Pd/Pt(II) benchmark complexes, but was still lower than that of the best lanthanide compounds based on phenolate macrocyclic ligands, reported by the group of Nakai. [10, 29, 31, 41, 42]

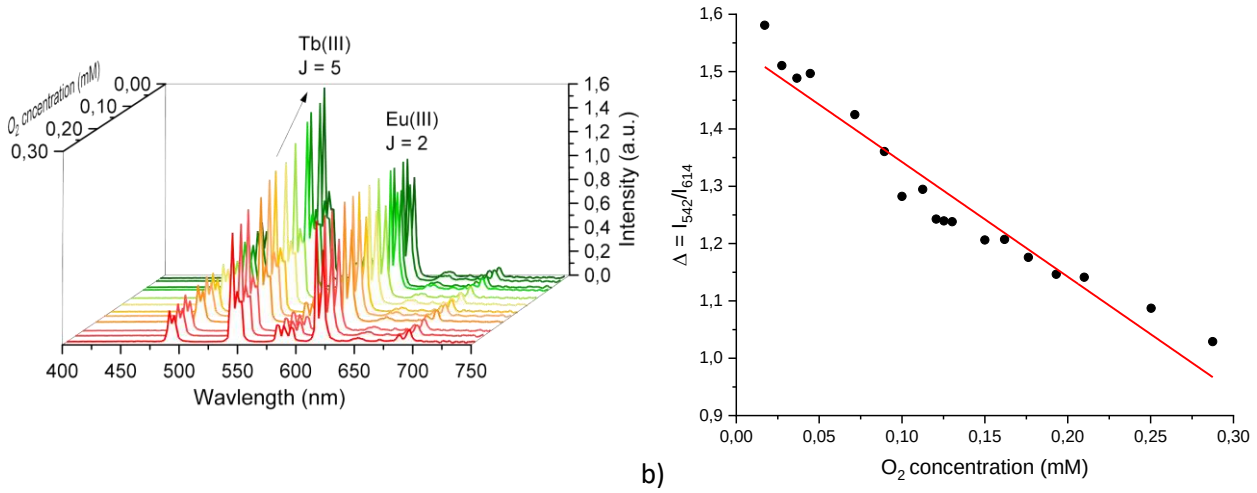

Figure 4. a) Variation of the luminescence of a **[TbL$_1$]**:[**EuL$_1$]** solution (2:1 mixture, H_2O, 293 K) as function of dissolved oxygen concentration. b) **Tb-to-Eu** emission intensity ratio (determined at 542 nm and 614 nm, respectively) *vs.* O_2 concentration.

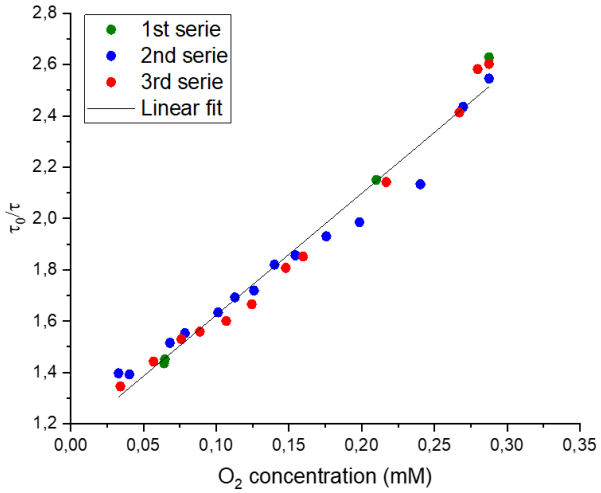

Figure 5. *Apparent* Stern-Volmer plot of the luminescence lifetime vs. oxygen concentration.

It is well-established that dioxygen sensitivity generally occurs through interaction with the triplet state of the antenna.[7, 43-45] During this process, a collision occurs between ground state dioxygen (triplet fundamental state $^3\Sigma$) and the excited antenna in its lowest-energy triplet state, which decreases the luminescence intensity and the lifetime of the emissive *f*- center. In degassed solution, this nonradiative deactivation pathway is suppressed and the luminescence is restored. Quenching by dioxygen is generally accompanied by the generation of singlet oxygen, although this aspect is implicit in many published studies. In the case of **[TbL$_1$]**, singlet oxygen was not observed when checking its characteristic NIR luminescence signal at 1270 nm in methanol or in dichloromethane.[46] Furthermore, EPR measurements carried out under irradiation did not reveal any traces of radicals, which might indicate the presence of reactive oxygen species and no degradation of the complex was

observed under irradiation, precluding photochemical reactions. Consequently, **[TbL$_1$]** appears to be sensitive to oxygen without the formation of singlet oxygen or ROS, possibly through $^1O_2$ quenching processes.[47, 48,49,50]

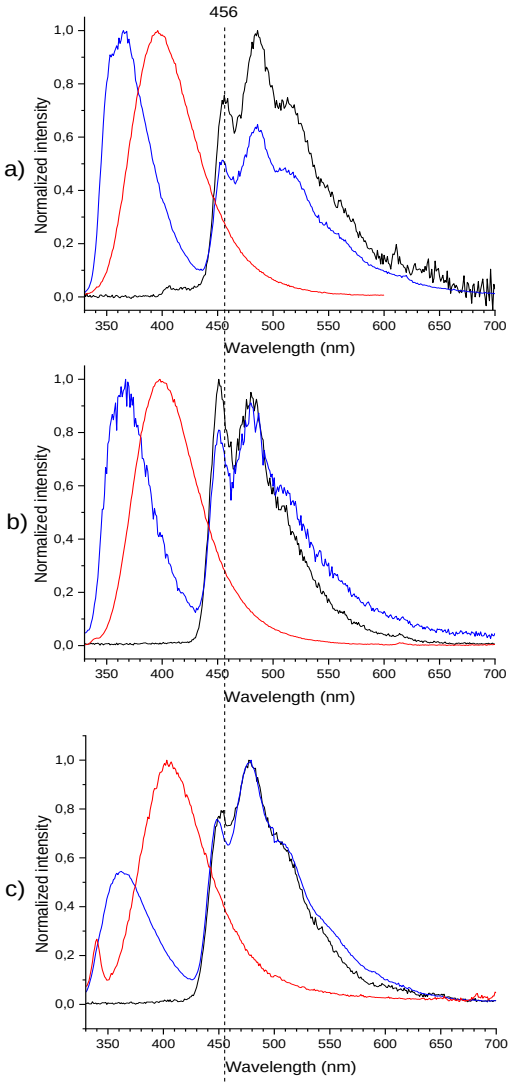

Figure 6. Emission spectra of a) **[GdL$_1$]** (λ_{ex} = 310 nm), b) **[GdL$_2$]** (λ_{ex} = 309 nm), c) **[GdL$_3$]** (λ_{ex} = 305 nm) in a EtOH/MeOH 4:1 (v/v) mixture, at ambient temperature (red) and 77 K (blue), and corresponding time-gated emission spectra at 77K (delay = 50 µs, black).

In order to gain more insight into the photophysics of the lanthanide probes, we then studied the related gadolinium(III) complexes **[GdL$_1$]**, **[GdL$_2$]**, and **[GdL$_3$]$^-$** in a EtOH/MeOH solution (4:1 v/v). At room temperature, only the blue ILCT fluorescence can be detected, centered at 400 nm for all complexes (Figure 6). At 77 K, a transparent, isotropic organic glass is formed and a dual emission is observed: a blue shifted singlet emission resulting from a local excited state (^{1}LE) and a red-shifted structured emission that remains intense using time-gated emission with a delay of 50 µs, assigned to the triplet phosphorescence.[46] The energy levels of the triplet excited state for the three complexes were determined from the 77 K emission spectra (Table 2) and the values were very similar for all three, comprised between 21900 and 22200 cm^{-1} for **[GdL$_1$]** and **[GdL$_3$]$^-$**, respectively.

In addition, it was possible to estimate the position of the singlet excited ILCT level, and for all complexes this position is almost identical (Table 2). Keeping in mind that the $^5D_4$ accepting state of Tb(III) is located at 20500 cm^{-1}, the energy difference with the triplet excited state was estimated to 1430, 1670 and 1720 cm^{-1} for **[TbL$_1$]**, **[TbL$_2$]** and **[TbL$_3$]$^-$**, respectively. This gap is in the range generally admitted for thermally-activated back-energy transfer to occur, enabling the repopulation of the ligand-centered triplet state from the $^5D_4$ terbium state.

Table 2. Photophysical data of **[GdL$_1$]**, **[GdL$_2$]**, **[GdL$_3$]$^-$**.

Complex	E_{ILCT} (cm^{-1})[a] ($\lambda_{on\text{-}set}$)	E_T (cm^{-1})[b]	τ[c] (µs)	τ^0 [d] (µs)	τ^0/τ
[GdL$_1$]	29 000	21 900	0.39	200	512
[GdL$_2$]	28 300	22 200	0.39	88	225
[GdL$_3$.]$^-$	28 200	22 200	0.53	470	886

a. measured in a mixture 4:1 EtOH/MeOH at room temperature, $\lambda_{on\text{-}set}$ is defined as the intersect of the tangent of the blue tail of emission curve at the inflection point with the X-axis. b. measured in a mixture 4:1 EtOH/MeOH at 77K, E_T is defined by the position of the first phosphorescence peak. c. measured in air-equilibrated MeOH at room temperature by TAS. d. measured in freeze-pump-thaw degassed MeOH solution at room temperature by TAS.

Finally, in order to gain a deeper insight into the triplet excited state quenching process, transient absorption spectroscopy (TAS) was performed on **[GdL$_1$]**, **[GdL$_2$]**, and **[GdL$_3$]$^-$** in MeOH solution under air and after degassing (Figure 7). In all cases, a triplet-triplet excited state absorption was observed peaking in the 450 and 500 nm range. Moreover, this triplet excited state presented a very long lifetime in degassed solutions (Table 2) ranging from 88 to 470 µs for the three different complexes. It should be noted that this lifetime is extremely sensitive to the quality of the degassing process and that even trace amounts of oxygen could lead to significant variations of these values. In Table 2 and Figure 7, we report the highest value obtained in sets of 3-5 different samples degassed by three freeze-pump-thaw cycles. Under air, the triplet lifetime decreased dramatically, reaching hundreds of ns (Table 2 and Figure S3). The τ^0/τ ratio of these gadolinium complexes was consequently very high reaching about 900 in the case of **[GdL$_3$]$^-$**. This value was far higher than that of the corresponding Tb(III) derivative (τ^0/τ = 2.6), indicating that energy transfer to the lanthanide ion decreases the sensitivity. This drawback is nevertheless compensated by an easier detection in the case of the Tb probe compared to Gd (luminescence emission vs TAS). It is also worth noting that such sensitivity is among the highest reported in the literature including transition metal complexes.[51]

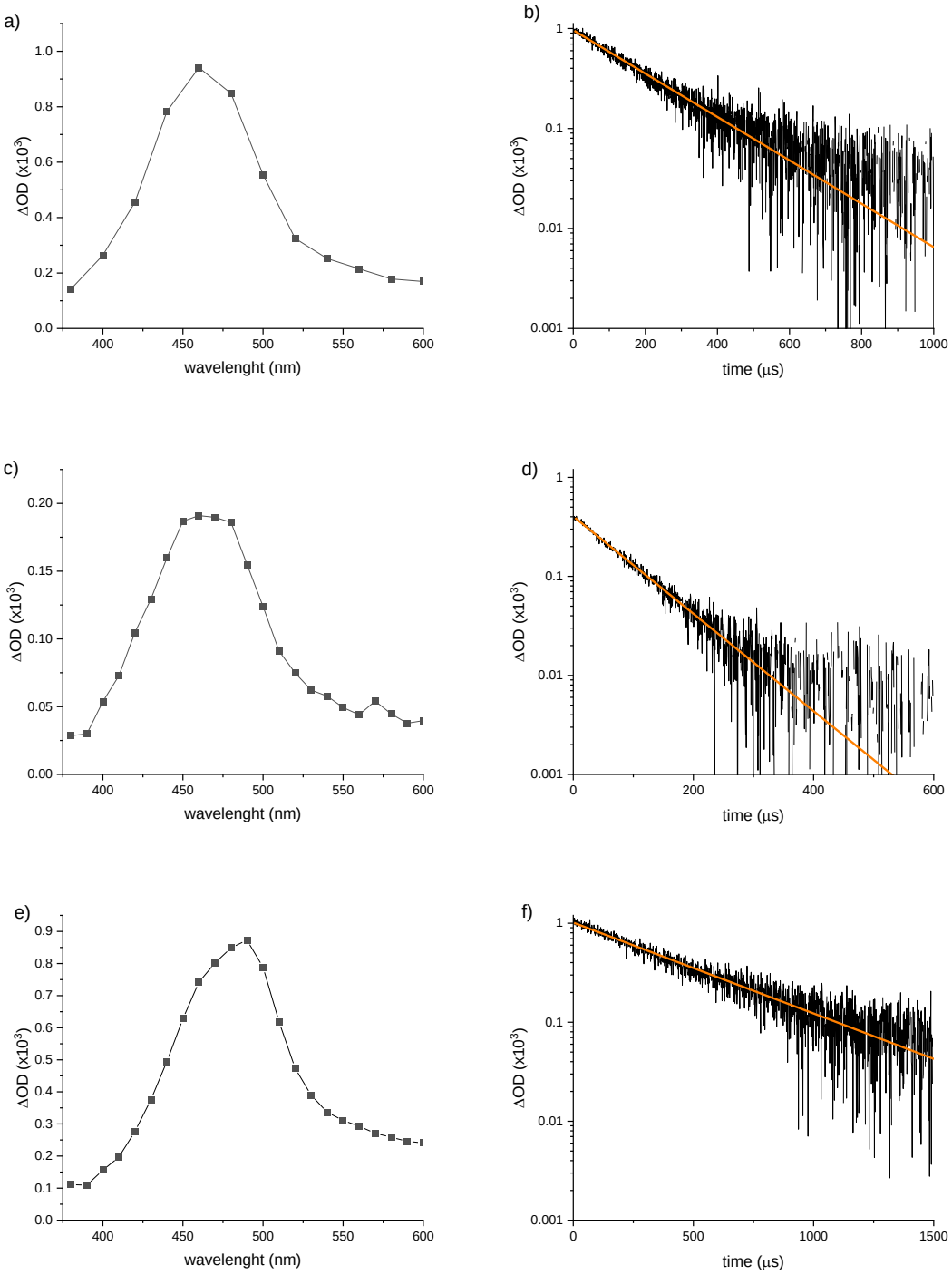

Figure 7. Transient absorption spectra (ΔOD) of **[GdL$_1$]** (at 10 μs, a), **[GdL$_2$]** (at 5 μs, c), and **[GdL$_3$]$^-$** (at 10 μs, e) MeOH solution previously degassed by freeze-pump-thaw cycles and corresponding transient absorption decay recorded at 450 nm (b), 460 nm (d) and 500 nm (f), respectively (λ_{ex} = 355 nm,E_{ex} = 25 μJ). In orange is represented the mono-exponential fit.

CONCLUSION

In conclusion, we reported herein the synthesis of lanthanide complexes based on different macrocyclic ligands (tacn, pyclen, cyclen) featuring the same anisolyl-picolinate antenna. This pendant chromophore rendered the corresponding Tb(III) complexes highly sensitive towards oxygen, while their Eu(III) analogues were steadily emissive regardless of the oxygen concentration in the medium. Such a contrasting behavior was explained by the presence of a thermally-activated back-energy transfer occurring only in the case of Tb(III). Thus, these complexes were perfectly suitable for the design of an oxygen ratiometric sensor system mixing Tb and Eu(III) complexes in a 2:1 ratio, or as lifetime based-Tb molecular probes in water. The sensitivity of these probes paves the way for *in cellulo* oxygen sensing applications. In addition, the sensitization mechanism was investigated using analogous Gd(III) complexes. Transient absorption spectroscopy revealed the exceptional sensitivity of the Gd-coordinated triplet excited state towards oxygen. These findings pave the way for the development of advanced luminescent sensors and bioprobes, offering promising opportunities for real-time oxygen monitoring in biological and environmental systems.

ASSOCIATED CONTENT

Supporting Information. Experimental section contains characterization of all new ligands and related complexes and air-equilibrated TAS data. This material is available free of charge via the Internet at http://pubs.acs.org."

AUTHOR INFORMATION

Corresponding Author

* olivier.maury@ens-lyon.fr

* olivier.seneque@cnrs.fr

* raphael.tripier@univ-brest.fr

Author Contributions

The manuscript was written through contributions of all authors. All authors have given approval to the final version of the manuscript. OM, OS, MB and RT designed and supervised the project. LB, LC, MH, ATB, KPM performed the synthesis; LB, ATB, OM and FR made the luminescence measurements and SRK, OM and AB the transient absorption spectroscopy.

Funding Sources

Part of this research was funded by the ANR program LANTEN (ANR-21-CE29-0018).

ACKNOWLEDGMENT

R.T., M. B. and L.C. acknowledge the Ministère de l'Enseignement Supérieur et de la Recherche (MESR) and the Centre National de la Recherche Scientifique and the Service Général des Plateformes of the University of Brest. Authors acknowledge Lhoussain Khrouz (LCH-ENS de Lyon) for running EPR experiments. ATB, MH, LB thank the MESR for the financial support, SRK; OM and AB acknowledge ANR 2LCDOR for a grant. OS acknowledges the Labex ARCANE, CBH-EUR-GS (ANR-17-EURE-0003).

REFERENCES

1. Heydari, E.; Yari, F.; Zare-Behtash, H., Vacuum Packaging Sensor Based on Time-Resolved Phosphorescence Spectroscopy. *Photonic Sensors* **2023,** *14* (1), 240120.
2. Lehner, P.; Staudinger, C.; Borisov, S. M.; Klimant, I., Ultra-sensitive optical oxygen sensors for characterization of nearly anoxic systems. *Nature Communications* **2014,** *5* (1), 4460.
3. Papkovsky, D. B.; Dmitriev, R. I., Imaging of oxygen and hypoxia in cell and tissue samples. *Cellular and Molecular Life Sciences* **2018,** *75* (16), 2963-2980.
4. Wang, X.-d.; Wolfbeis, O. S., Optical methods for sensing and imaging oxygen: materials, spectroscopies and applications. *Chem. Soc. Rev.* **2014,** *43* (10), 3666-3761.
5. Kautsky, H., Energie-Umwandlungen an Grenzflächen, IV. Mitteil.: H. Kautsky und A. Hirsch: Wechselwirkung zwischen angeregten Farbstoff-Molekülen und Sauerstoff. *Berichte der deutschen chemischen Gesellschaft (A and B Series)* **1931,** *64* (10), 2677-2683.
6. Effects of Intermolecular Photophysical Processes on Fluorescence Emission. In *Molecular Fluorescence*, 2001; pp 72-124.
7. Zhao, X.; Liu, J.; Fan, J.; Chao, H.; Peng, X., Recent progress in photosensitizers for overcoming the challenges of photodynamic therapy: from molecular design to application. *Chem. Soc. Rev.* **2021,** *50* (6), 4185-4219.
8. Pham, T. C.; Nguyen, V.-N.; Choi, Y.; Lee, S.; Yoon, J., Recent Strategies to Develop Innovative Photosensitizers for Enhanced Photodynamic Therapy. *Chem. Rev.* **2021,** *121* (21), 13454-13619.
9. Sivakumar, R.; Lee, N. Y., Recent advances in luminescent lanthanides and transition metal complex-based probes for imaging reactive oxygen, nitrogen, and sulfur species in living cells. *Coord. Chem. Rev.* **2024,** *501*, 215563.
10. Kitagawa, Y.; Nakai, T.; Hosoya, S.; Shoji, S.; Hasegawa, Y., Luminescent Lanthanide Complexes for Effective Oxygen-Sensing and Singlet Oxygen Generation. *ChemPlusChem* **2023,** *88* (6), e202200445.
11. Reddy, M. L. P.; Bejoymohandas, K. S., Luminescent lanthanide-based molecular materials: applications in photodynamic therapy. *Dalton Transactions* **2024,** *53* (5), 1898-1914.
12. Young, S. W.; Woodburn, K. W.; Wright, M.; Mody, T. D.; Fan, Q.; Sessler, J. L.; Dow, W. C.; Miller, R. A., Lutetium Texaphyrin (PCI-0123): A Near-Infrared, Water-Soluble Photosensitizer. *Photochem. Photobiol.* **1996,** *63* (6), 892-897.
13. Johnson, K. R.; Lombardi, V. C.; de Bettencourt-Dias, A., Photocytotoxicity of Oligothienyl-Functionalized Chelates That Sensitize LnIII Luminescence and Generate 1O2. *Chemistry – A European Journal* **2020,** *26* (52), 12060-12066.
14. Zhang, J. X.; Chan, W. L.; Xie, C.; Zhou, Y.; Chau, H. F.; Maity, P.; Harrison, G. T.; Amassian, A.; Mohammed, O. F.; Tanner, P. A.; Wong, W. K.; Wong, K. L., Impressive near-infrared brightness and singlet oxygen generation from strategic lanthanide-porphyrin double-decker complexes in aqueous solution. *Light Sci Appl* **2019,** *8*, 46.
15. Galland, M.; Le Bahers, T.; Banyasz, A.; Lascoux, N.; Duperray, A.; Grichine, A.; Tripier, R.; Guyot, Y.; Maynadier, M.; Nguyen, C.; Gary-Bobo, M.; Andraud, C.; Monnereau, C.; Maury, O., A "Multi-Heavy-Atom" Approach toward Biphotonic Photosensitizers with Improved Singlet-Oxygen Generation Properties. *Chemistry* **2019,** *25* (38), 9026-9034.

16. Ke, X. S.; Ning, Y.; Tang, J.; Hu, J. Y.; Yin, H. Y.; Wang, G. X.; Yang, Z. S.; Jie, J.; Liu, K.; Meng, Z. S.; Zhang, Z.; Su, H.; Shu, C.; Zhang, J. L., Gadolinium(III) Porpholactones as Efficient and Robust Singlet Oxygen Photosensitizers. *Chemistry* **2016,** *22* (28), 9676-86.
17. Yang, Z.-S.; Yao, Y.; Sedgwick, A. C.; Li, C.; Xia, Y.; Wang, Y.; Kang, L.; Su, H.; Wang, B.-W.; Gao, S.; Sessler, J. L.; Zhang, J.-L., Rational design of an "all-in-one" phototheranostic. *Chemical Science* **2020,** *11* (31), 8204-8213.
18. Zhu, M.; Zhang, H.; Ran, G.; Mangel, D. N.; Yao, Y.; Zhang, R.; Tan, J.; Zhang, W.; Song, J.; Sessler, J. L.; Zhang, J.-L., Metal Modulation: An Easy-to-Implement Tactic for Tuning Lanthanide Phototheranostics. *Journal of the American Chemical Society* **2021,** *143* (19), 7541-7552.
19. Xie, C.; Chau, H.-F.; Zhang, J.-X.; Tong, S.; Jiang, L.; Fok, W.-Y.; Lung, H.-L.; Zha, S.; Zou, R.; Jiao, J.; Ng, C.-F.; Ma, P. a.; Zhang, J.; Lin, J.; Shiu, K. K.; Bünzli, J.-C. G.; Wong, W.-K.; Long, N. J.; Law, G.-L.; Wong, K.-L., Bladder Cancer Photodynamic Therapeutic Agent with Off-On Magnetic Resonance Imaging Enhancement. *Advanced Therapeutics* **2019,** *2* (11), 1900068.
20. Jenni, S.; Sour, A., Molecular Theranostic Agents for Photodynamic Therapy (PDT) and Magnetic Resonance Imaging (MRI). *Inorganics* **2019,** *7* (1), 10.
21. Abad Galán, L.; Hamon, N.; Nguyen, C.; Molnár, E.; Kiss, J.; Mendy, J.; Hadj-Kaddour, K.; Onofre, M.; Trencsényi, G.; Monnereau, C.; Beyler, M.; Tircsó, G.; Gary-Bobo, M.; Maury, O.; Tripier, R., Design of polyazamacrocyclic Gd3+ theranostic agents combining magnetic resonance imaging and two-photon photodynamic therapy. *Inorganic Chemistry Frontiers* **2021,** *8* (9), 2213-2224.
22. D'Aléo, A.; Pointillart, F.; Ouahab, L.; Andraud, C.; Maury, O., Charge transfer excited states sensitization of lanthanide emitting from the visible to the near-infra-red. *Coord. Chem. Rev.* **2012,** *256* (15-16), 1604-1620.
23. Sorensen, T. J.; Kenwright, A. M.; Faulkner, S., Bimetallic lanthanide complexes that display a ratiometric response to oxygen concentrations. *Chem Sci* **2015,** *6* (3), 2054-2059.
24. Steemers, F. J.; Verboom, W.; Reinhoudt, D. N.; van der Tol, E. B.; Verhoeven, J. W., New Sensitizer-Modified Calix[4]arenes Enabling Near-UV Excitation of Complexed Luminescent Lanthanide Ions. *Journal of the American Chemical Society* **1995,** *117* (37), 9408-9414.
25. Quici, S.; Marzanni, G.; Forni, A.; Accorsi, G.; Barigelletti, F., New Lanthanide Complexes for Sensitized Visible and Near-IR Light Emission: Synthesis, 1H NMR, and X-ray Structural Investigation and Photophysical Properties. *Inorg. Chem.* **2004,** *43* (4), 1294-1301.
26. Lehr, J.; Tropiano, M.; Beer, P. D.; Faulkner, S.; Davis, J. J., Ratiometric oxygen sensing using lanthanide luminescent emitting interfaces. *Chem Commun (Camb)* **2015,** *51* (88), 15944-7.
27. Hueting, R.; Tropiano, M.; Faulkner, S., Exploring energy transfer between pyrene complexes and europium ions – potential routes to oxygen sensors. *RSC Adv.* **2014,** *4* (83), 44162-44165.
28. Law, G. L.; Pal, R.; Palsson, L. O.; Parker, D.; Wong, K. L., Responsive and reactive terbium complexes with an azaxanthone sensitiser and one naphthyl group: applications in ratiometric oxygen sensing in vitro and in regioselective cell killing. *Chem Commun (Camb)* **2009,** (47), 7321-3.
29. Nakai, H.; Seo, J.; Kitagawa, K.; Goto, T.; Matsumoto, T.; Ogo, S., An oxygen-sensitive luminescent Dy(iii) complex. *Dalton Trans* **2016,** *45* (23), 9492-6.
30. Nakai, H.; Seo, J.; Kitagawa, K.; Goto, T.; Nonaka, K.; Matsumoto, T.; Ogo, S., Control of Lanthanide Coordination Environment: Synthesis, Structure, and Oxygen-Sensitive Luminescence Properties of an Eight-Coordinate Tb(III) Complex. *Inorg. Chem.* **2016,** *55* (13), 6609-15.
31. Nakai, H.; Kuyama, M.; Seo, J.; Goto, T.; Matsumoto, T.; Ogo, S., Luminescent Tb(iii) and Sm(iii) complexes with a 1,4,7-triazacyclononane-based tris-aryloxide ligand for high-performance oxygen sensors. *Dalton Trans* **2017,** *46* (28), 9126-9130.
32. Thor, W.; Kai, H.-Y.; Yeung, Y.-H.; Wu, Y.; Cheung, T.-L.; Tam, L. K. B.; Zhang, Y.; Charbonnière, L. J.; Tanner, P. A.; Wong, K.-L., Unearthing the Real-Time Excited State Dynamics from Antenna to Rare Earth Ions Using Ultrafast Transient Absorption. *JACS Au* **2024,** *4* (10), 3813-3822.
33. Bui, A. T.; Grichine, A.; Duperray, A.; Lidon, P.; Riobe, F.; Andraud, C.; Maury, O., Terbium(III) Luminescent Complexes as Millisecond-Scale Viscosity Probes for Lifetime Imaging. *J. Am. Chem. Soc.* **2017,** *139* (23), 7693-7696.

34. Bui, A. T.; Roux, A.; Grichine, A.; Duperray, A.; Andraud, C.; Maury, O., Twisted Charge-Transfer Antennae for Ultra-Bright Terbium(III) and Dysprosium(III) Bioprobes. *Chemistry* **2018,** *24* (14), 3408-3412.
35. Bui, A. T.; Grichine, A.; Duperray, A.; Lidon, P.; Riobé, F.; Andraud, C.; Maury, O., Correction to "Terbium(iii) Luminescent Complexes as Millisecond-Scale Viscosity Probes for Lifetime Imaging". *Journal of the American Chemical Society* **2018,** *140* (25), 8048-8048.
36. Walter, E. R. H.; Williams, J. A. G.; Parker, D., Solvent polarity and oxygen sensitivity, rather than viscosity, determine lifetimes of biaryl-sensitised terbium luminescence. *Chem. Commun.* **2017,** *53* (100), 13344-13347.
37. Le Fur, M.; Beyler, M.; Molnar, E.; Fougere, O.; Esteban-Gomez, D.; Tircso, G.; Platas-Iglesias, C.; Lepareur, N.; Rousseaux, O.; Tripier, R., The role of the capping bond effect on pyclen natY3+/90Y3+ chelates: full control of the regiospecific N-functionalization makes the difference. *Chem. Commun. (Cambridge, U. K.)* **2017,** *53* (69), 9534-9537.
38. Le Fur, M.; Beyler, M.; Molnar, E.; Fougere, O.; Esteban-Gomez, D.; Tircso, G.; Platas-Iglesias, C.; Lepareur, N.; Rousseaux, O.; Tripier, R., Stable and Inert Yttrium(III) Complexes with Pyclen-Based Ligands Bearing Pendant Picolinate Arms: Toward New Pharmaceuticals for β-Radiotherapy. *Inorg. Chem.* **2018,** *57* (4), 2051-2063.
39. Malikidogo, K. P.; Charnay, T.; Ndiaye, D.; Choi, J. H.; Bridou, L.; Chartier, B.; Erbek, S.; Micouin, G.; Banyasz, A.; Maury, O.; Martel-Frachet, V.; Grichine, A.; Seneque, O., Efficient cytosolic delivery of luminescent lanthanide bioprobes in live cells for two-photon microscopy. *Chem Sci* **2024,** *15* (25), 9694-9702.
40. Binnemans, K., Interpretation of europium(III) spectra. *Coord. Chem. Rev.* **2015,** *295*, 1-45.
41. Nakai, H.; Goto, T.; Kitagawa, K.; Nonaka, K.; Matsumoto, T.; Ogo, S., A highly luminescent and highly oxygen-sensitive Tb(iii) complex with a tris-aryloxide functionalised 1,4,7-triazacyclononane ligand. *Chem. Commun.* **2014,** *50* (99), 15737-15739.
42. Nakai, H.; Nonaka, K.; Goto, T.; Seo, J.; Matsumoto, T.; Ogo, S., A macrocyclic tetraamine bearing four phenol groups: a new class of heptadentate ligands to provide an oxygen-sensitive luminescent Tb(III) complex with an extendable phenol pendant arm. *Dalton Trans* **2015,** *44* (24), 10923-7.
43. Pandya, S.; Yu, J.; Parker, D., Engineering emissive europium and terbium complexes for molecular imaging and sensing. *Dalton Trans* **2006,** (23), 2757-66.
44. Parker, D.; Fradgley, J. D.; Wong, K. L., The design of responsive luminescent lanthanide probes and sensors. *Chem. Soc. Rev.* **2021,** *50* (14), 8193-8213.
45. Nguyen, V. N.; Yan, Y.; Zhao, J.; Yoon, J., Heavy-Atom-Free Photosensitizers: From Molecular Design to Applications in the Photodynamic Therapy of Cancer. *Acc. Chem. Res.* **2021,** *54* (1), 207-220.
46. Gallavardin, T.; Maurin, M.; Marotte, S.; Simon, T.; Gabudean, A. M.; Bretonniere, Y.; Lindgren, M.; Lerouge, F.; Baldeck, P. L.; Stephan, O.; Leverrier, Y.; Marvel, J.; Parola, S.; Maury, O.; Andraud, C., Photodynamic therapy and two-photon bio-imaging applications of hydrophobic chromophores through amphiphilic polymer delivery. *Photochem Photobiol Sci* **2011,** *10* (7), 1216-25.
47. Gsponer, H. E.; Previtali, C. M.; García, N. A., Evidence for physical quenching of singlet oxygen (O2(1Δg)) by dinitrophenols. *Journal of Photochemistry* **1987,** *36* (3), 247-253.
48. Tamura, H.; Ishikita, H., Quenching of Singlet Oxygen by Carotenoids via Ultrafast Superexchange Dynamics. *The Journal of Physical Chemistry A* **2020,** *124* (25), 5081-5088.
49. Schmidt, R.; Shafii, F., Influence of Charge Transfer Interactions on the Sensitization of Singlet Oxygen: Formation of O2(1Σg+), O2(1Δg), and O2(3Σg-) during Oxygen Quenching of Triplet Excited Biphenyl Derivatives. *J. Phys. Chem. A* **2001,** *105*, 8871-8877.
50. Schweitzer, C.; Mehrdad, Z.; Noll, A.; Grabner, E.-W.; Schmidt, R., Mechanism of Photosensitized Generation of Singlet Oxygen during Oxygen Quenching of Triplet States and the General Dependence of the Rate Constants and Efficiencies of O2(1Σg+), O2(1Δg), and O2(3Σg-) Formation on Sensitizer Triplet State Energy and Oxidation Potential. *The Journal of Physical Chemistry A* **2003,** *107* (13), 2192-2198.
51. Wang, X. D.; Wolfbeis, O. S., Optical methods for sensing and imaging oxygen: materials, spectroscopies and applications. *Chem. Soc. Rev.* **2014,** *43* (10), 3666-761.